JOURNAL OF MATERIALS SCIENCE **35** (2000) 4667–4672

Positron lifetime measurements for characterization of nano-structural changes in the age hardenable AlCuMg 2024 alloy

T. E. M. STAAB*
Martin-Luther Universität Halle-Wittenberg, Fachbereich Physik, Friedemann-Bach-Platz 6, D-06108 Halle/Saale, Germany
E-mail: tst@fyslab.hut.fi

E. ZSCHECH‡
Daimler-Crysler Aerospace, Airbus GmbH EVM, D-28183 Bremen, Germany

R. KRAUSE-REHBERG
Martin-Luther Universität Halle-Wittenberg, Fachbereich Physik, Friedemann-Bach-Platz 6, D-06108 Halle/Saale, Germany

We investigate the changes in the microstructure on a nano-scale (nano-structure) in technically used AlCuMg 2024 alloys. We show how the annihilation parameters, i.e. the positron lifetimes and corresponding intensities, are changing during natural and artificial aging. It turns out that positron annihilation spectroscopy is very sensitive to changes occurring in the nano-structure but which are not always reflected or measurable in the materials properties such as hardness. The detected changes in the positron lifetime, corresponding to trapping at precipitations, indicate transport of copper atoms through the aluminum matrix to the precipitations. Multi-component spectra for very long aging times indicate that the distances between the trapping centers have increased. This means that the precipitations grow in size, while their number decreases.

1. Nano-sized microstructure — the key for custom tailored aluminum materials

The phenomenon of particle hardening in aluminum alloys was discovered by Wilm in the year 1906, investigating AlCuMg alloys of different chemical composition [1]. The explanation for this accidental discovery was given by Guinier and Preston in the late 30th [2, 3]. During natural or artificial aging, ordered microstructural regions — so-called Guinier-Preston zones (GP zones) — and meta stable phases are formed in age-hardenable aluminum alloys. They hinder dislocation movement effectively and, hence, are causing increasing hardness [4, 5]. This means that custom tailoring of material properties, by applying a defined heat treatment, is possible [6].

Microstructure analysis on a nano-scale, called *nano-structure* in the following, as well as knowledge about the correlation between nano-structure and macroscopic material properties are indispensable for the development of new aluminum alloys. This information is of particular interest for solving specific problems on the one hand, and for characterization of eventually occurring changes of the material under realistic conditions on the other hand [7].

The characterization of the nano-structure of aluminum alloys requires the complex application of different physical analysis techniques. Transmission electron microscopy (TEM) has been developed to an efficient "tool" which provides not only images and diffraction patterns but enables also an element analysis of particular regions of the microstructure (EDS or EFTEM, EELS) down to a range of nanometers.

Using TEM, it is possible to characterize morphology, crystalline structure, and chemical composition of different microstructural regions [8]. The information obtained from individual parts of the microstructure can be combined with complementary integral investigation methods which scan a large number of microstructural parts and, hence, allow statistical statements about the material. Examples are X-ray methods like small angle scattering, diffuse scattering, and X-ray absorption spectroscopy, but also positron annihilation spectroscopy (PAS).

In recent years, positron annihilation spectroscopy has become a powerful tool for the investigation of defect-structures in solid state physics. It has been shown that this technique can be used for characterization of the microstructure in age-hardenable aluminum

* *Present Address*: Helsinki University of Technology, Laboratory of Physics, P.O. Box 1100, FIN-02015 HUT, Finland.
‡ *Present Address*: AMD Saxony Manufacturing GmbH, Materials Analysis Department, P.O. Box 11 01 10, D-01330 Dresden, Germany.

materials (AlZnMg: [9–12], AlCuMg: [13–15], AlLi: [16, 17], AlSc: [18] — see also [19] for a review).

The aim of this article is to point out the following relations for AlCuMg alloys systematically:

- The influence of the chemical composition of the precipitations in the alloys on the average positron lifetime, and determination of the positron lifetimes for different types of precipitations (decomposition of the spectra).
- Influence of artificial aging on the positron lifetime in AlCuMg alloys.
- Influence of natural aging on the positron lifetime in AlCuMg alloys.

2. Positron interaction with precipitations

The advantage of nano-structural studies of solids by positron annihilation relies on the fact that kinetic investigations can be performed *in situ* and non-destructively. Furthermore, one obtains statistical data averaged among a great number of precipitations in the alloys, since positron annihilation is an integral method. Hence, the information drawn from that is complementary to TEM results.

2.1. Interaction of positrons with defects

Positron lifetime spectroscopy (POLIS) and Doppler broadening spectroscopy of the annihilation line (DOBS) have been applied to investigate vacancy-type defects in solid state physics for about 25 years. Usually, the β^+ irradiation from ^{22}Na is used as a positron source. The radioactive Sodium isotope decays to an exited state of ^{22}Ne under the emission of a positron. Within a few ps, the excited state of the Ne atom decays to the ground state under emission of a γ quantum (1.274 MeV). In positron lifetime spectroscopy, this γ quantum is detected as starting signal. The positron penetrating the sample loses its initial energy of up to 540 keV within a few ps mainly by inelastic collisions with electrons. When the positron has slowed down to thermal energies of $3/2k_BT$, it is starting a diffusive motion through the sample. During this random walk motion, the positron is elastically scattered by phonons. The maximum penetration depth during thermalization is up to some 100 μm (The medium penetration depth is — depending on the charge of the nuclei — 15–60 μm) while the average positron diffusion length, given by $L_+ = \sqrt{2dD_+\tau_{\text{eff}}}$ [20], is about 400 nm in defect-free Al. Here d is the dimension of the diffusive motion, D_+ is the material specific positron diffusion constant, and $1/\tau_{\text{eff}} = \lambda_{\text{eff}} = \lambda_b + \mu C_d$ is the reciprocal of the effective positron lifetime — the effective annihilation rate (μ is the trapping coefficient — being material and defect specific, C_d the defect concentration, and λ_b the annihilation rate in the perfect crystal). The diffusion length determines the sensitivity of the investigation technique. If the defects, e.g. vacancies or dislocations, are so far apart that nearly no positron, i.e. less than 2%, is able to reach the defects on its diffusion path, then this determines the lower sensitivity limit. If nearly all, i.e. more than 98% of all positrons, are reaching defects, then this determines the upper sensitivity limit (see [21] for a review). This is similar for evenly distributed nano-sized precipitations in the matrix.

In the undisturbed crystal (bulk) the positron stays — after thermalization — mainly in the interstitial regions, i.e. far away from the positively charged nuclei. It annihilates preferentially with valence electrons after a material specific lifetime of $\tau_b \approx 158$ ps for Al. This positron lifetime is determined by the electron density at the annihilation site. The emitted annihilation radiation of two 511-keV γ quanta is detected in positron lifetime spectroscopy as a stop signal. Other parameters which can be measured are the angular correlation of the emitted γ quanta and their Doppler broadening. From the former the Fermi surface can be determined since the momentum of the positron is small in comparison to that of the electrons. DOBS can be used for investigations of the microstructure. It reveals information about the momentum distribution at the annihilation site of the positrons and, hence, is sensitive to the chemical environment in Al-alloys [22, 23].

If vacancies are present in the solid in a sufficiently high concentration, a measurable amount of positrons is localized at the vacancy sites, because the positive core is missing at this point, and because the electron clouds of the surrounding atoms spread into the vacancy site, creating locally a negative charge. Hence, an attractive potential exists for the positron at the vacancy site. The simplest approximation would be a three-dimensional square potential. This means the positron is in a quantum mechanically bound state. Since the electron density at the place where the positron is localized will be smaller than in defect-free areas, the annihilation probability or the annihilation rate λ_v will be lower, i.e. the lifetime $\tau_v = 1/\lambda_v$ will be longer (approximately $\tau_v \approx 240$ ps for monovacancies in Al). Hence, POLIS is able to separately detect vacancy-like defects with different electron densities. This means, the defects usually have different spatial extension and, hence, different electron densities: like monovacancies, vacancy clusters, or surface states (defect-related lifetimes for positrons trapped to surface states are known to be $\tau_{\text{surf}} \approx 500$–$600$ ps for Al [24, 25]). Positron trapping due to interstitial atoms or non-negatively charged impurities or anti-structure defects is not detected. Depending on the binding energy, positrons can escape thermally activated from traps having a small binding energy for positrons. This could be the bare dislocation line in Al or its alloys [26–28]. In Al alloys, principally, also coherent precipitations could act as shallow positron traps.

2.2. Setup for lifetime measurements

The measurement of the positron lifetime is based on the time difference between the birth of the positron (simultaneous emission of the start-γ quanta) and the annihilation radiation (stop-γ quanta). As given schematically in Fig. 1, a so-called *source-sample-sandwich* arrangement is used where the positron source is placed between two identical samples.

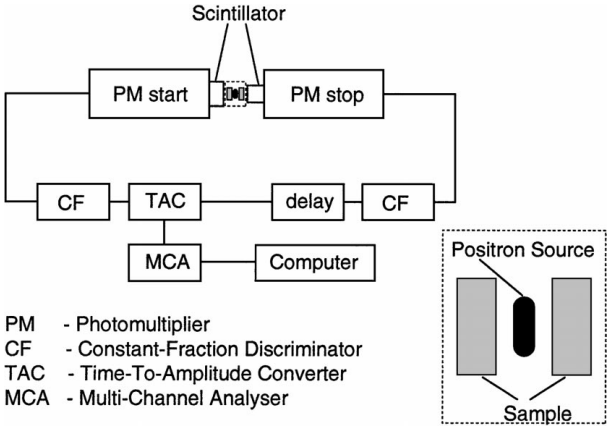

Figure 1 Principle of lifetime measurement: the source-sample arrangement is magnified.

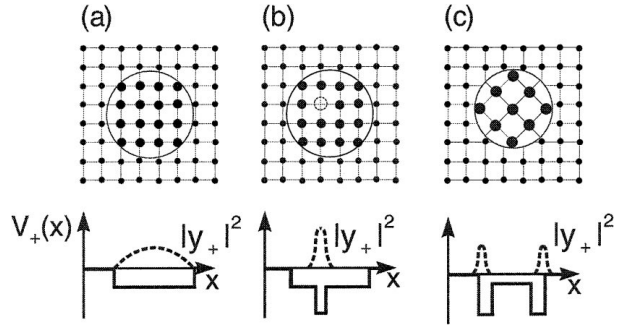

Figure 2 Possible capture of positrons in or at precipitations ((a): coherent, (b): coherent containing structural vacancies, (c): in-coherent): Shown is also the attractive potential felt by the positrons and which causes the binding. The position probability density, i.e. the positron wave function squared (dashed line), is given as well.

Constant-fraction discriminators are in use for the detectors within a fast-fast coincidence setup. One of the detectors has its energy window set to the start-γ, and the other to the stop-γ quantum. Only coincident events will be accepted. The γ-quanta are creating scintillation light in the plastic scintillators which is amplified proportional to the initial energy of the quanta by the following photo multipliers. The energy selection is done by the constant fraction discriminators. By choosing appropriate energy windows, it can be made sure that no stop-incidents are registered as start-incidents. Otherwise, the energy windows should be the best possible compromise between a good time resolution (FWHM $\approx$ 250 ps) and an acceptable counting rate ($\approx$500–800 s^{-1}). From the start and stop incidents, the time-to-amplitude converter shows a voltage proportional to the time between the detected radiation quanta. The single events are stored in a multi-channel analyzer according to the time measured. The experimental lifetime spectrum is convoluted with the time-resolution function of the setup. Since a deconvolution is numerically very difficult, a model spectrum is created, and using a non-linear Gauß-Newton-Marquardt regression procedure, the lifetimes and intensities of the function are fitted to the experimental data (for reviews cf. e.g. [23, 29, 30]).

2.3. Interaction of positrons with precipitations

There are different possibilities of a positron interaction with coherent or incoherent precipitations. If the positron affinity A of the precipitation is higher than that of the surrounding matrix, the positron can be trapped even into totally coherent precipitations, i.e. where no 'open volume' is existing. Hence, the corresponding lifetime will be that of the corresponding intermetallic phase. One additional condition for this is that the precipitation is larger than a critical size [31]. All elements typically used in Al alloys (Li (second row in periodic table), Mg, Si (third row), Sc, Zn, Cu (fourth row), Ag (fifth row)) have a significant larger positron affinity A than pure aluminum [32]. This means, at precipitations, in which these elements are concentrated, there is an attractive potential for positrons. Examples are $A_{Mg} - A_{Al} = -1.77$ eV and $A_{Cu} - A_{Al} = -0.40$ eV. Furthermore, positron lifetime spectroscopy is able to give additional information on the type of the precipitation: coherent, semi-coherent, incoherent, or coherent but containing structural vacancies (cf. Fig. 2). Especially the transition from totally coherent to semi-coherent precipitations can be monitored well using positron annihilation. This can be seen from the decomposition of the spectra [9, 22]. Combining lifetime measurements with Doppler broadening investigations, additional information can be obtained about the chemical environment of the annihilation place (nearest neighbor atoms to the trapping center). In coherent precipitations, the positron wave function is delocalized over the whole spatial extension of the precipitation, while in the semi- or in-coherent case, the wave function is localized at the misfit dislocations in the precipitation-matrix interface or at the interface itself (cf. Fig. 2). Hence, the annihilation parameters change significantly. Since an incoherent precipitation has a defect-rich interface to the Al matrix, which is comparable to grain boundaries, the positron will certainly be localized at the interface. We give some examples for the sensistivity of POLIS in Table I.

2.4. The trapping model

The trapping model has been thoroughly described in a recent review [21] (cf. also [23]). Therefore, we give only the special features for positron trapping to precipitations in this paper. One of the basic assumptions in using the standard trapping model (STTM) is that positron trapping centers have to be evenly distributed in the matrix. The trapping itself can be rate or diffusion limited — depending on the kind of trap. The

TABLE I Annihilation parameters for different radii r and different average distances d of precipitations in Al calculated according to Equation 2. Here, κ is the trapping rate and η_2 the fraction of trapped positrons

τ_{eff} [nm]	d [nm]	κ [s^{-1}]	η_2
1	7.4	10^{13}	0.999
10	74.2	10^{11}	0.940
100	742.17	10^{9}	0.136
1000	7416.9	10^{7}	0.0016

STTM leads to different data analysis then the diffusion trapping model (DTM), proposed in the case of trapping at grain boundaries [33], i.e. not evenly distributed defects.

The result of an analysis according to the STTM are the trapping rates κ_i ($i = 2, 3, \ldots$), related for rate limited capture to the defect density as follows:

$$\kappa_i = \mu_i C_i, \tag{1}$$

where μ_i is the trapping coefficient which is temperature independent for vacancies in metals [20]. This is valid up to temperatures just below the melting point [34].

Since, in the case of extended defects like precipitations, the trapping is diffusion limited, a different expression than (1) is obtained. This means that the diffusion of the positron to the defect is the limiting factor for the trapping, and not the capture rate. For nearly spherical defects,

$$\kappa_i = \frac{4\pi D_+ r_{\text{eff}}}{\Omega} C_i; \quad \eta_i = \frac{\kappa_i \tau_b}{1 + \tau_b \sum_{j=2} \kappa_j} \tag{2}$$

is obtained where D_+ is the diffusion constant for positrons ($D_+ = (1.7 \pm 0.2)$ cm^2 s^{-1} for Al at room temperature [35]), r_{eff} is the effective radius of the capturing center, Ω is the atomic volume, and C_i is the defect concentration per atom for defect i. $N_i = C_i / \Omega$ is the defect concentration per volume, being, in the case considered here, the number $N = 6/(\pi d^3)$ of precipitations per volume, where d is the average distance of the capture centers. We consider here Equation 2 only for $i = 2$ meaning only one type of defect in the samples [21]. Intensity I_2 and trapping fraction are plotted in Fig. 3 in depence on trapping rate, vacancy concentration, dislocation density or precipitation distance. In this case, the trapping coefficient is temperature dependent via D_+: $\mu \propto T^{1/2}$ for low and $\mu \propto T^{-1/2}$ for higher temperatures (cf. [36] and references therein, e.g. [37]).

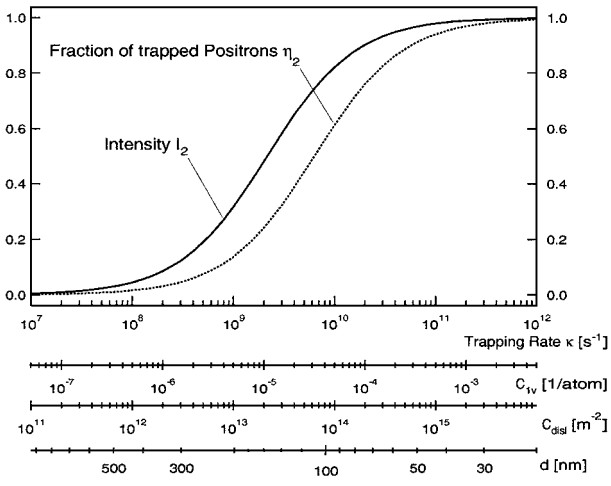

Figure 3 Only one defect-related lifetime component: given are the intensity I_2 corresponding to the defect-related lifetime component and the fraction of trapped positrons η_2 in dependence on the capture rate κ_2, as well as the corresponding concentration of monovacancies C_{1v}, dislocations C_d, and the average distance d between precipitations assumed to have a radius of 2 nm.

Since one can generally not expect complete trapping to defects of one kind (e.g. vacancies) one has to decompose also the Doppler spectra to obtain the annihilation line for positrons trapped to defects. Therefore, it is absolutely necessary to combine Doppler broadening and lifetime measurements, since the average lifetime $\bar{\tau}$ as well as the momentum distribution of the electron positron pair are linear combinations of annihilation events in the bulk (index 'b') and in vacancies (index 'v'):

$$\bar{\tau} = (1 - \eta_v)\tau_b + \eta_v \tau_v \tag{3}$$

$$f(p_z) = (1 - \eta_v)\, f_b(p_z) + \eta_v\, f_v(p_z), \tag{4}$$

where η_v is the fraction of positrons annihilating in vacancies, and $f(p_z)$ the momentum distribution of the annihilating positron. Equation 4 is often written with the apparent S parameter [23]:

$$S = (1 - \eta_v) S_b + \eta_v S_v. \tag{5}$$

From Equation 3 and 4 or 5, f_v can be obtained if f_b or S_b are known, since POLIS determines all unknown values in (3).

3. Experimental results

The investigated samples were cut from sheets of the AlCuMg aircraft alloy 2024. The protecting Al plating was removed by etching.

Then, the samples were investigated using positron lifetime spectroscopy. In nearly all cases we did find only single-component spectra. Since the lifetime related to trapping in precipitations (about 200 ps) is significantly above the bulk lifetime in the undisturbed Al matrix (about 158 ps), the precipitations seem to contain vacancy-like defects which are trapping the positrons. The positron lifetime of about 210 ps in the initial state is significantly below that one measured for monovacancies in pure Al (about 240 ps), but certainly above the corresponding value for vacancies in pure copper (about 170 ps) [21]. The changes of the average lifetime from the initial state with increasing aging time can be explained by further transport of copper atoms to the precipitations. Since copper has a relatively small bulk lifetime, i.e. 112 ps, the average lifetime for positrons trapped to precipitations is decreasing by copper diffusing to and incorporation into the precipitations (compare Figs 4–6). So, the chemical composition of the precipitations is changed.

Fig. 4 shows the change of the positron lifetime during natural aging up to 40 years. The straight line is a linear fit to the experimental points in a logarithmic scale of the time axis. Figs 5 and 6 correspond to artificial aging at 85 and 130°C, respectively. The higher the applied temperatures the faster are the diffusion processes. This fact corresponds to the detected positron lifetimes, decreasing much more rapidly for higher aging temperature.

In the figures only the average lifetime is show, since the attempt to perform a multi-component decomposition of the spectra was impossible for shorter aging times and failed also for the largest aging time.

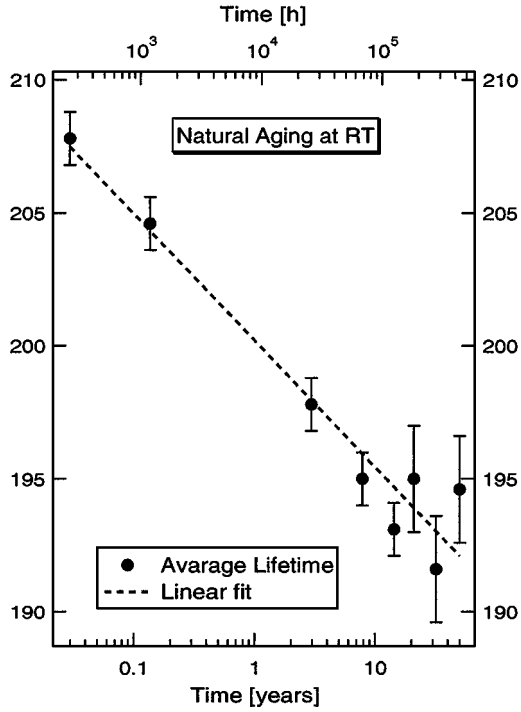

Figure 4 Change of the average positron lifetime with the duration of natural ageing of the 2024 T3 alloy.

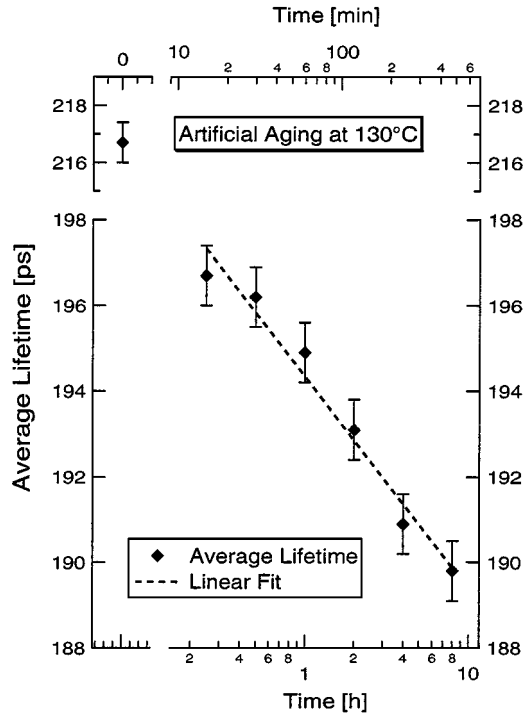

Figure 6 Changes of the average positron lifetime with the duration of artificial aging the 2024 T3 alloy at 130°C.

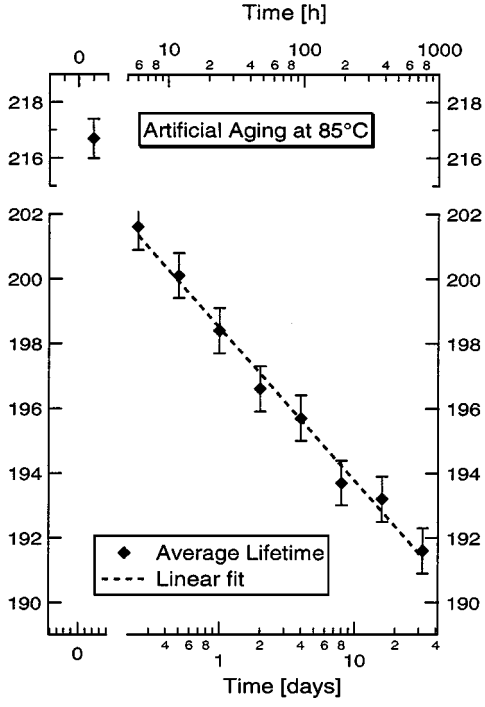

Figure 5 Change of the average positron lifetime with the duration of artificial aging of the 2024 T3 alloy at 85°C.

Even though, the spectrum analysis showed that for the longest aging time there must be more than one single component, it was not possible to extract this from experimental data accurately. This is probably due to small differences in the expected lifetimes [38] and perhaps the fact that only a too small fraction of positrons is not trapped.

We measured the Doppler broadening of the annihilation radiation simultaneously to POLIS. The values for the *S* parameter change similarly to the average lifetime, i.e. they decrease exponentially with time (not shown in the figures). The decrease up to values significantly below the annihilation parameters related to trapping at vacancies in Al supports the explanation by Cu atom diffusion to the precipitations.

4. Conclusions

Since sample preparation and TEM studies are very time consuming[§], the investigation is usually limited to certain chosen exemplary sample states. With help of positron annihilation measurements, it is possible to study solid-state physical processes in technical materials, e.g. changes in the nano structure of Al alloys during aging, with reasonable effort and statistically broader basis.

For the 2024 aluminum aircraft alloy, it turns out that the average positron lifetime decreases continuously with time during aging at room temperature and artificial aging (85°C, 130°C). This means the nano structure is changed even by natural aging over very long periods of time (>10 years). But no changes in the micro hardness could be measured. It could not be determined any changes in static mechanical properties as well as in damage-tolerance properties.

Since we detected complete trapping of the positrons to the precipitations (single component spectra) in nearly all experiments, the average distance of the precipitations can be estimated to be less than about 50 nm if an average radius of 2 nm is assumed. This is according to Equation 2 assuming that more than 98% of the positrons are trapped (cf. also Fig. 3). The detected positron lifetimes, corresponding to trapping to precipitations (about 200 ps), are significantly above the bulk

[§] Good statistical statements are only possible spending a lot of time.

lifetime of the undisturbed Al matrix (158 ps). Since this is valid for pure Al-Cu alloys as well, vacancy-like defects in the precipitations seem to be responsible for the detected positron lifetime. The increasing copper content shows up in a decreasing positron lifetime, since the positron lifetime related to defects in bulk copper, i.e. vacancies, is much smaller than the corresponding one in Al or Mg. Simultaneously to the decreasing positron lifetime, the measured *S* parameter decreases as well. This result is reasonable since the *S* parameter for Cu is smaller than that for Al.

Summarizing, the positron lifetime is a signal responding very sensitively to changes in the microstructure. The interpretation of the results from the metallurgical point of view is that the coherent particles being fine-disperse in the matrix are growing with increasing aging time and hence the total energy of the system is reduced. The copper content is increased in the particles and a depletion of copper in the matrix is observed.

Growth of precipitations means that their average distance increases as well. For very long aging times, this process results in the fact that the lifetime spectra seem to be no more single component. Consequently, a measurable fraction of the positrons reaches no more the precipitations on its diffusion way and, hence, a significant part of the positrons annihilates in the undisturbed Al matrix. But even for the longest aging time considered, the fraction of positrons annihilating in the Al matrix stays so small that it cannot be separated accurately from the defect-related annihilation events.

Acknowledgement

The authors thank E. Loechelt (Daimler-Crysler Aerospace Airbus GmbH) for valuable comments and U. Hornauer (Forschungszentrum Rossendorf) for interesting discussions and comments on the manuscript.

References

1. A. WILM, *Metallurgie* **8** (1911) 255.
2. A. GUINIER, *Ann. Phys.* **12** (1938) 161.
3. G. D. PRESTON, *Phil. Mag.* **26** (1938) 855.
4. E. HORNBOGEN and H. WARLIMONT, "Metallkunde" (Springer Verlag, Berlin, 1991).
5. P. HAASEN, *Physikalische Metallkunde*. 2nd. edi. (Springer Verlag, Berlin, 1984).
6. E. ZSCHECH, *HTM* **51**(3) (1996) 137.
7. G. PETZOW and F. MÜCKLICH, *Prakt. Met. Sonderbd.* **26** (1995) 29.
8. D. B. WILLIAMS, In Proc. 4th Int. Conf. on Aluminum Alloys, Vol. 3, Atlanta, 1994, edited by T. H. Sanders and E. A. Starke, p. 50.
9. G. DLUBEK, O. BRÜMMER and R. KRAUSE, Positron studies of vacancies and Guinier-Preston zones in Al-Zn and Al-Zn-Mg alloys. *Crys. Res. Technol.* **20** (1985) 275.
10. G. DLUBEK, R. KRAUSE, O. BRÜMMER and F. PLAZAOLA, *J. of Materials Sci.* **21** (1986) 853.
11. R. FERRAGUT, A. SOMOZA and A. DUPASQUIER, *J. Phys.: Condens. Matter* **8** (1996) 8945.
12. *Idem., ibid.* **10** (1998) 3903.
13. U. GLÄSER, G. DLUBEK and R. KRAUSE, *Phys. Stat. Sol. (a)* **163** (1991) 337.
14. G. DLUBEK, H. KRAUSE, S. KRAUSE, R. UNGER and W. HEYROTH, *ibid. (a)* **169** (1998) R11.
15. G. DLUBEK, P. LADEMANN, H. KRAUSE, S. KRAUSE and R. UNGER, *Scr. Materialia* **39** (1998) 893.
16. G. DLUBEK, S. KRAUSE, H. KRAUSE, A. L. BERESINA, V. S. MIKHALENKOV and K. V. CHUISTOV, *J. Phys.: Condens. Matter* **4** (1992) 6317.
17. J. DELRIO, N. DE DIEGO and F. PLAZAOLA, *ibid.* **10** (1998) 5327.
18. S. KRAUSE, G. DLUBEK, H. KRAUSE, A. L. BERESINA, K. V. CHUISTOV and V. S. MIKHALENKOV, *Phys. Stat. Sol. (a)* **141** (1994) 311.
19. A. DUPASQUIER, P. FOLEGATI, N. DE DIEGO and A. SOMOZA, *J. Phys.: Condens. Matter* **10** (1998) 10409.
20. R. M. NIEMINEN, Defect and surface studies with positrons. in Proceedings of the International School of Physics "Enrico Fermi" – Positron Solid State Physics, North Holland, Amsterdam, 1983. edited by W. Brandt and A. Dupasquier, p. 359.
21. T. E. M. STAAB, R. KRAUSE-REHBERG and B. KIEBACK, *J. Materials Sci.* **34** (1999) 3833.
22. R. KRAUSE, *Untersuchungen zum Entmischungsverhalten von aushärtbaren Al-Legierungen mit Hilfe der Positronenannihilation.* Dissertation, Fakultät für Naturwissenschaften der Martin-Luther-Universität Halle-Wittenberg, Fachbereich Physik, Fr.-Bach-Platz 6, D-06108 Halle/Saale, Germany, 1985.
23. R. KRAUSE-REHBERG and H. S. LEIPNER, "Defects in Semiconductors," 1st ed. (Springer Verlag, Berlin, Heidelberg, 1999).
24. K. G. LYNN, W. E. FRIEZE and P. J. SCHULTZ, *Phys. Rev. Lett.* **52**(13) (1984) 1137.
25. R. M. NIEMINEN, M. J. PUSKA and M. MANNINEN, *ibid.* **53**(13) (1984) 1298.
26. H. S. LEIPNER, C. G. HÜBNER, T. E. M. STAAB, M. HAUGK and R. KRAUSE-REHBERG, *Phys. Stat. Sol. (a)* **171** (1999) 377.
27. L. C. SMEDSKJAER, M. MANNINEN and M. J. FLUSS, *J. Phys. F: Metal Phys.* **10** (1980) 2237.
28. H. HÄKKINEN, S. MÄKINEN and M. MANNINEN, *Phys. Rev.* **B41**(18) (1990) 12441.
29. P. HAUTOJÄRVI, "Positrons in Solids, Topics in Current Physics," Vol. 12 1st ed. (Springer Verlag, Berlin, Heidelberg, 1979).
30. W. BRANDT and A. DUPASQUIER, (eds). in Proceedings of the International School of Physics "Enrico Fermi" – Positron Solid State Physics, North Holland, Amsterdam, 1983.
31. G. BISCHOF, V. GRÖGER, G. KREXNER and R. M. NIEMINEN, *J. Phys.: Condens. Matter* **8** (1996) 7523.
32. M. J. PUSKA, P. LANKI and R. M. NIEMINEN, *ibid.* **1** (1989) 6081.
33. A. DUPASQUIER, R. ROMERO and A. SOMOZA, *Phys. Rev.* **B48**(13) (1993) 9235.
34. J. E. KLUIN and TH. HEHENKAMP, *ibid.* **B44**(11) (1991) 597.
35. E. SOININEN, H. HUOMO, P. A. HUTTUNEN, J. MÄKINEN, A. VEHANEN and P. HAUTOJÄRVI, *ibid.* **B41**(10) (1990) 6227.
36. T. MCMULLEN, in "Positron Annihilation," edited by P. C. Jean, R. M. Singru, and K. P. Gopinathan (World Scientific, Singapore, 1985) p. 822.
37. B. BERGENSEN, E. PAJANNE, P. KUBICA, M. J. STOTT and C. H. HODGES, *Solid State Commun.* **15** (1974) 1377.
38. B. SOMIESKI, T. E. M. STAAB and R. KRAUSE-REHBERG, *Nucl. Instr. and Meth.* **A381** (1996) 128.

Received 20 May 1999
and accepted 3 February 2000